JOURNAL OF CATALYSIS **164,** 232–245 (1996)
ARTICLE NO. 0378

The Adsorption of NO and Reaction of NO with O_2 on H-, NaH-, CuH-, and Cu-ZSM-5: An *in Situ* FTIR Investigation

János Szanyi and Mark T. Paffett

Chemical Science and Technology Division, Los Alamos National Laboratory, CST-18, MS J-565, Los Alamos, New Mexico 87545

Received March 18, 1996; revised July 16, 1996; accepted July 17, 1996

The adsorption of NO and the reaction of NO with O_2 on H-, NaH-, CuH-, and Cu-ZSM-5 zeolites were studied at 300 K using *in situ* Fourier transform infrared spectroscopy (FTIR). At this temperature, NO readily adsorbs on the Cu^+ sites of CuH- and Cu-ZSM-5 catalysts and decomposition of NO is observed for all catalysts, although the rate of decomposition is vastly different on these materials. In comparison, this reaction is negligible over the H- and NaH-ZSM-5 samples. The time evolution of several nitrogen-containing molecules after controlled O_2 exposure to the NO/ZSM-5 systems has allowed the spectral correlation of these species. These nitrogen-containing species can interact with either the protonic sites of bridging hydroxyls forming hydrogen bonding complexes or the metal cations producing primarily surface nitrates and nitrites. The hydrogen bonded N_xO_y complexes were characterized with their IR absorption features: (a) NO_2, 2133 cm^{-1}; (b) N_2O_3, 1875 and 1587 cm^{-1}; and (c) N_2O_4, 2185 and 1745 cm^{-1}. The stretching vibrational frequency of the acidic OH groups of ZSM-5 red-shifts due to the interaction with nitrogen-containing molecules and forms "ABC" band structures characteristic of medium and strong hydrogen bonding complexes. Although the adsorbed N_xO_y species (N_2O_3, N_2O_4) interacting with the Brønsted protons exhibit characteristics of a strong Lewis base, adsorption enthalpies are sufficiently weak that their existence is not observed even after brief evacuation. Nitric oxide, oxygen coadsorption produces metal cation (Na^+ and Cu^{n+}) bonded surface species possessing IR absorption bands between 1400 and 1650 cm^{-1} characteristic of nitrite and nitrate species. The thermal stability of the nitrite and nitrate adsorbed species is much greater than the N_xO_y species nucleated at free Brønsted acid sites.

INTRODUCTION

The adsorption and conversion of NO as well as the reaction of NO with other molecules have attracted a great deal of attention in recent years due to their importance in the catalytic removal of NO_x from automotive exhaust. Overexchanged Cu-ZSM-5 zeolites have shown the most promising catalytic properties for the reduction of NO in oxygen-rich environments (1–18). Among a series of reactions that ultimately lead to the reduction of NO to N_2 and O_2, the formation of NO_2 via the reaction of NO and O_2 has been suggested to be a key reaction step (19). High activity for the $NO + O_2$ reaction over H-ZSM-5 has also been reported (19, 20). From the large body of experimental data collected on the catalytic reduction of NO_x, the importance of both the MFI zeolite structure and the nature of the charge compensating cations are reviewed as very important parameters in comparing reactivity differences. Despite the significant advances made recently, many mechanism related questions remain unanswered. *In situ* IR spectroscopy has widely been used in most of the mechanistic studies of selective catalytic reduction (SCR) of NO_x. This is done usually to establish correlations among the surface species (observed either under real high-temperature reaction conditions or at lower temperatures) and the catalytic properties of the catalysts (1, 3, 7, 8, 21–30). Unfortunately, under high-temperature reaction conditions most of the possible intermediates have residence times on the surface (or in the catalyst itself) so short that observing them with IR spectroscopy becomes tenous. Adsorption measurements and reaction studies performed at relevant partial pressures and at room temperature and below and reaction studies can provide valuable information about the existence of adsorbed surface species participating in the SCR process. However, extreme care must be taken when conclusions about reaction mechanisms are inferred from extrapolating low-temperature observations to high-temperature real catalytic conditions.

Despite the large number of vibrational spectroscopic investigations on Cu-ZSM-5, a number of observed IR absorption features still have ambiguous assignments. In NO decomposition studies carried out over ion exchanged Cu-ZSM-5 catalysts the only well characterized features are those representing Cu^{1+} and Cu^{2+} bound NO molecules. Because of the complex nature of the NO decomposition reaction, a number of adsorbed N_xO_y species form in the absence of gas-phase oxygen. Oxygen, originating from the NO decomposition reaction, can react with NO molecules to produce NO_2. Copper-bound oxygen species can also contribute to the formation of NO_2 molecules. At low temperatures in the presence of NO/O_2 gas mixture, NO_2 is formed in equilibrium amounts. The presence of a series of N_xO_y species opens up the possibility of the formation of

0021-9517/96 $18.00

a number of adsorbed species which may play important roles in the selective catalytic reduction of NO_x by hydrocarbons. The formation of these N_xO_y entities, however, is not restricted to Cu-containing zeolites. They have, indeed, been shown to form over other zeolites (e.g., Na-, Ca-, H-form Y, FAU) by the disproportionation of NO ($3NO \Leftrightarrow N_2O + NO_2$ and $4NO \Leftrightarrow N_2O_3 + N_2O$) (31, 32). All of these N_xO_y species can then interact with specific sites within the catalyst, forming adsorbed entities with intrinsically different reactivities. Thus, the spectroscopic characterization of the development of these species formed in the absence and presence of gas-phase oxygen on zeolite catalysts in different cationic provides a sufficient motivation for their study.

In this study, we report results obtained in the investigation of the adsorption of NO and the reaction of NO with O_2 on two basic sets of catalysts, using *in situ* FTIR spectroscopy. One of the catalyst materials (Cu-ZSM-5) contained no bridging hydroxyl groups eliminating the possibility of the contribution of Brønsted acidic protonic sites to either the adsorption or the reaction. The other group of catalysts (H-, NaH-, and CuH-ZSM-5) have the common feature of containing protonic sites and also metal cations in charge compensating positions. The role of these protonic centers in the development of many widely observed spectral features will be established and discussed.

EXPERIMENTAL

The experiments were performed in a home-built IR cell consisting of a turbomolecularly pumped 2.75-in. conflat six-way cross with CaF windows. The cell was mounted in the sample compartment of a Mattson Cygnus 100 FTIR spectrometer equipped with an MCT detector. Typically the spectrometer operated at 4 cm^{-1} resolution collecting 256 scans in a single-beam mode. Background spectra were collected on the clean adsorbate-free samples to eliminate the overlap of IR absorption features that originate from the zeolite structural vibrations and the adsorbed surface species. The powder samples were pressed onto a tungsten wire mesh, which enabled us to heat the sample resistively up to 1200 K. The sample temperature was monitored using a chromel/alumel thermocouple spot-welded to the top center of the tungsten mesh. The sample prepared this way was mounted onto a specially designed stainless-steel sample holder. This assembly was attached to metal to ceramic feed-through welded to a double-wall sample manipulator rod. The rod with the sample attached to it was connected to a linear motion translator, enabling positioning of the sample in and out of the IR beam. The IR cell was connected to a complete gas manifold system for gas cleaning, storing, and/or providing precise flow of gases regulated by mass flow controllers.

The parent Na-ZSM-5 zeolite was provided by PQ Corporation and had an Si/Al ratio of 16. For the preparation of H-, NaH-, and CuH-ZSM-5 catalysts the solution ion exchange method was used, while the proton-free Cu-ZSM-5 sample was prepared by solid-state ion exchange of an H-ZSM-5 material with CuCl. The H-ZSM-5 sample was prepared from the parent Na-ZSM-5 material using a multiple ion exchange (3×8 h) with a 0.1 mol/liter NH_4F solution at 350 K, followed by washing with deionized water until no F^- ions were detected in the effluent. The NaH- and CuH-ZSM-5 catalysts were prepared by following the same protocol using $NaNO_3$ and Cu(II)-acetate solutions. After ion exchange the samples were first dried at room temperature and then at 373 K under flowing nitrogen. The zeolite sample was mounted as described above and the organic residues left behind either from the zeolite synthesis or from ion exchange were removed at 700 K in the presence of 2 Torr of oxygen for 1 h. The sample was then annealed at 900 K until the base pressure dropped below 1×10^{-6} Torr. For the Cu,H-ZSM-5 catalyst this procedure ensured the conversion of all Cu^{2+} ions into Cu^{1+} via autoreduction. Thus, in the Cu,H-ZSM-5 sample all the copper centers are present in the +1 oxidation state. After this calcination step, the sample was cooled back to room temperature and its cleanliness was verified by IR spectroscopy. All the IR measurements were conducted at a sample temperature of 300 K.

A proton-free Cu-ZSM-5 sample was prepared by solid-state ion exchange of H-ZSM-5 with CuCl. The solid-state ion exchange was carried out in a quartz tube reactor attached to a vacuum line. The parent NH_4-ZSM-5 sample was first slowly heated up to 850 K and annealed at this temperature for 6 h. This treatment resulted initially in the slow, systematic dehydration followed by the deammoniation of the ammonium form ZSM-5. The sample then was cooled back to room temperature and removed from the reactor. Cuprous chloride in an amount larger than that needed for the quantitative ion exchange of protons for Cu^+ ions was placed on the bottom of the quartz reactor. Then a thin layer of quartz wool was positioned on the top of the CuCl to prevent direct contact between CuCl and H-ZSM-5. The deammoniated H-ZSM-5 sample was then placed into the reactor, and finally it was capped with a thick layer of quartz wool to protect the zeolite powder from being sucked out of the vacuum line upon degassing and also to prevent deposition of CuCl vapor in the vacuum line. The reactor prepared this way was first evacuated and then slowly heated up to about 400 K and kept at this temperature overnight to ensure the removal of adsorbed water from both the zeolite and the CuCl. Then the reactor temperature was raised to 700 K to provide a sufficient CuCl vapor pressure for the solid-state ion exchange. The reactor was kept at this temperature for 6 h and then it was heated up to 900 K to ensure the removal of all excess CuCl from the reaction zone.

Analytical characterization of both major constituents and minor impurities for the zeolite materials in different ion exchanged forms was accomplished using glow discharge mass spectrometry (GDMS), inductively coupled plasma mass spectroscopy, X-ray fluorescence, and atomic emission spectroscopy. The elemental ratios for the samples are as follows: H-ZSM-5: Si/Al = 22.7; Na-ZSM-5: Si/Al = 22.7, Na/Al = 0.9; Cu,H-ZSM-5: Si/Al = 21.3, Cu/Al = 0.4; Cu-ZSM-5: Si/Al = 27.9, Cu/Al = 2.2.

The reactants NO and O_2 were research grade purity purchased from Matheson. Before use NO was passed through a silica-filled trap cooled with dry ice/acetone slurry to remove other nitrogen oxide impurities. The oxygen was used as received without any further purification. The adsorption and reaction studies were carried out in batch reactor mode. First, a certain amount of NO was introduced into the IR cell at a sample temperature of 300 K. IR spectra were collected for 60 min to follow the decomposition of NO on these materials at room temperature. After 60 min of NO decomposition, oxygen was dosed into the cell and the reaction was followed by IR for 20 min. Subsequent additional oxygen doses were introduced twice more and the reaction was followed by IR for 20 min after each oxygen dose. Finally, the cell was evacuated for 10 min and the sample was checked with IR to identify the surface species strongly adsorbed on the catalysts during the room temperature reaction.

RESULTS AND DISCUSSION

H-ZSM-5

The adsorption and conversion of NO and the reaction of NO with O_2 was first investigated on the H-ZSM-5 sample to establish the possible role of protonic sites in these processes. At room temperature following a 10 Torr NO exposure, NO does not adsorb on the protonic sites of H-ZSM-5 zeolite due to the weak interaction between NO and the protons (CO behaves similarly). As Fig. 1 demonstrates, the most intense IR absorption feature in the spectrum of NO on H-ZSM-5 is that of the gas phase NO at 1876 cm^{-1}. There are some other IR features due to impurities or product N_2O (~2250 cm^{-1}) and the products of the very slow decomposition of NO on H-ZSM-5 (2133, 1814, 1628, and 1463 cm^{-1}). The intensities of all the IR features change very little during the 60 min reaction time suggesting that NO itself does not react on the H-ZSM-5 catalyst under the conditions of this study. The intensity of the 2250 cm^{-1} band somewhat decreases, while the peaks at 2133, 1814, and 1630 cm^{-1} increase parallel with each other. The very small intensity increases of these features suggests that the conversion of NO is occuring on other metallic portions of the sample cell (e.g., on the copper heating legs of the feed-through). Furthermore, these features may originate from N_xO_y species formed by the disproportionation of NO ($3NO \Leftrightarrow N_2O + NO_2$ and $4NO \Leftrightarrow N_2O_3 + N_2O$), as was

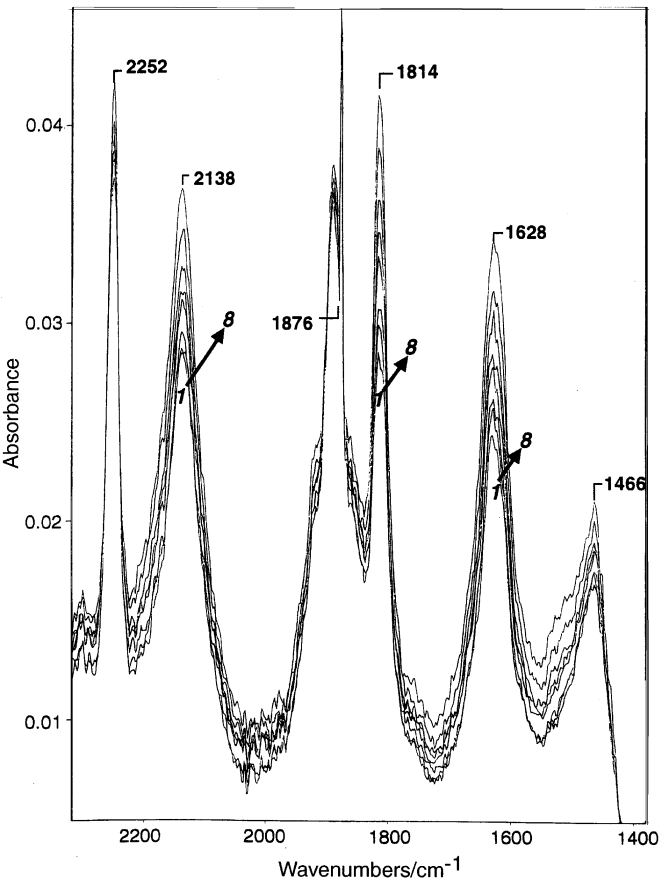

FIG. 1. IR spectra obtained from H-ZSM-5 in the presence of NO. Spectra were collected at reaction times 0, 5, 10, 15, 20, 30, 45, and 60 min [$T = 300$ K; $P_{NO} = 10.23$ Torr].

suggested by Lunsford *et al.* over Na-, Ca-, H- and decationated Y, FAU zeolites (31, 32). The intensity increase of the 2133 cm^{-1} band is correlated with the decrease in intensity of the Brønsted acidic OH groups. This observation is in good agreement with that reported by Hoost *et al.* (21). Introducing a small aliquot of oxygen (much less than that required to convert all the NO into NO_2) into the IR cell after the 60 min NO reaction results in the development of several very intense IR absorption features. Immediately after the introduction of the first oxygen dose a very sharp intensity increase of the 2133 cm^{-1} feature is observed (Fig. 2A) and concomitantly the intensity of the 3615 cm^{-1} band decreases (Fig. 2B). As the intensity of the 3615 cm^{-1} feature decreases, two new, very broad features centered at 2485 and 2905 cm^{-1} develop, as shown in Fig. 2B. These bands correspond to the vibrations of O–H groups interacting with a moderate to strongly basic molecule.

These broad, H-bonded O–H features were reported to be absent on a CuH-ZSM-5 sample in interaction with NO, NO_2 and an $NO + O_2$ reactant gas mixture (21). This observation is surprising since the authors presented conclusive evidence that NO_2 indeed interacted with Brønsted

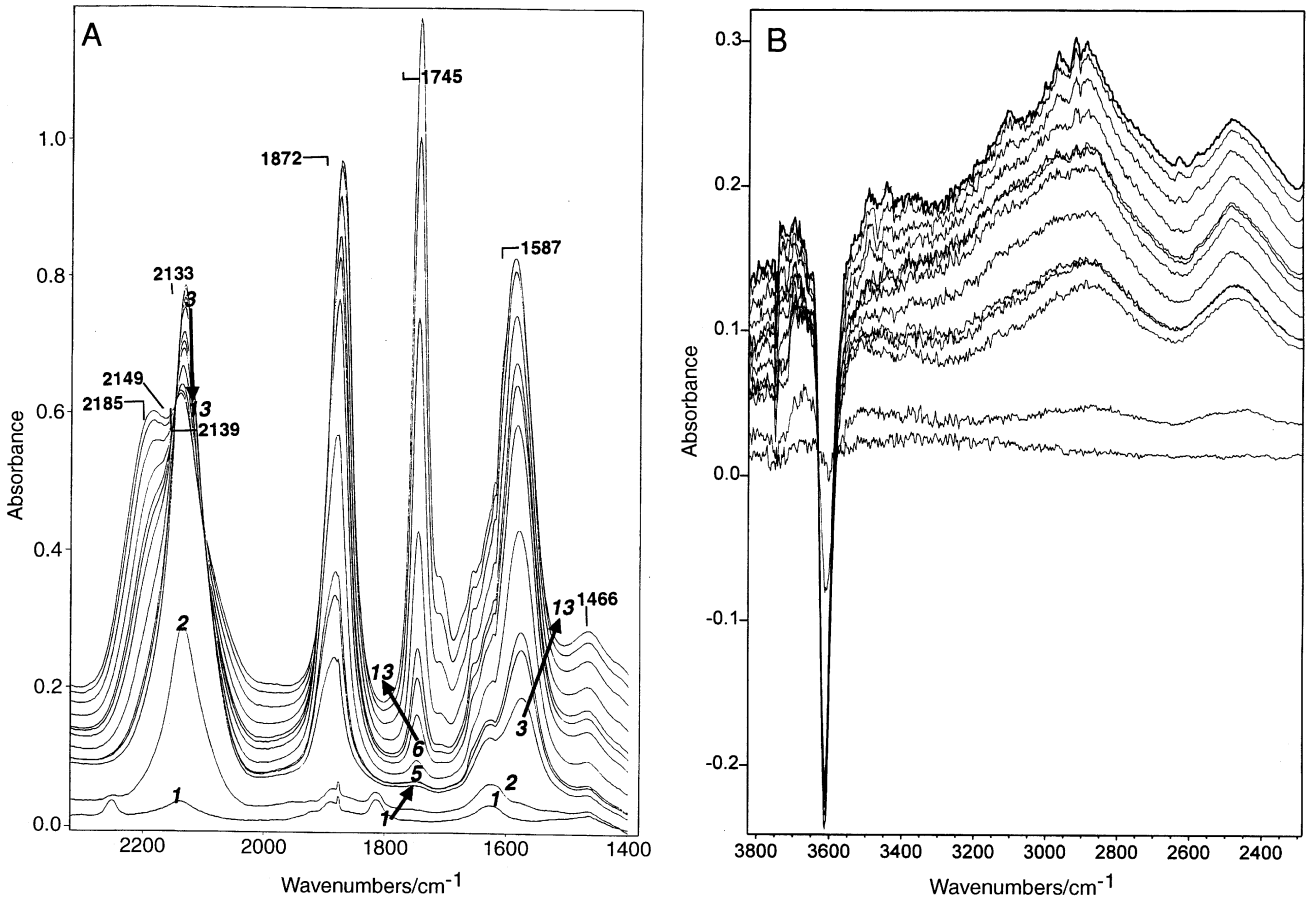

FIG. 2. IR spectra obtained from H-ZSM-5 in the presence of $NO + O_2$ in the 1400–2350 cm^{-1} (A) and 2400–3800 cm^{-1} (B) regions. Spectra 1: at t = 60 min in NO; 2–5: 1 + first oxygen dose ($P_{O_2} = 0.53$ Torr) (0, 5, 10, and 20 min); 6–9: 5 + second dose of oxygen ($P_{O_2} = 1.10$ Torr) (0, 5, 10, and 20 min); 10–13: 9 + third oxygen dose ($P_{O_2} = 1.96$ Torr) (0, 5, 10, and 20 min) [$P_{NO(initial)} = 10.23$ Torr; $T = 300$ K].

acidic OH groups. This interaction was shown to result in the decrease of the 3615 cm^{-1} IR band as it reacted with NO_2 (21). The claim of the absence of the shifted OH features could only be rationalized by the assumption that for the adsorbate–OH interaction complete proton transfer takes place from the bridging acidic OH groups to the adsorbate (formation of ion pairs as is seen for the interaction of ammonia with H-form zeolites, e.g., $Z{-}O{-}H + NH_3 \rightarrow Z{-}O^- + NH_4^+$). However, complete proton transfer reactions are only expected when the acidic OH groups react with very strong bases (e.g., NH_3 or pyridine). The chemical species expected to be present in the $NO + O_2$ system are not considered as strong bases and therefore a weaker hydrogen bonding interaction between adsorbates and the protonic acid sites is observed. In Ref. 21 (Fig. 7 spectrum C), the complete disappearance of the 3615 cm^{-1} vibrational band of the acidic OH groups is shown, which should produce lower frequency, shifted OH bands. The absence of these shifted OH bands in Ref. (21) is potentially explained by the comparatively small number of bridging hydroxyl groups in the starting Cu-ZSM-5 material and the intrinsically low intensity arising from these H-bonding interactions making them difficult to observe.

The scientific basis and literature on the interaction of basic molecules with OH groups of medium to strong acidities producing very broad IR features designated as an "ABC" structure is well established (33–43). The "ABC" band structure of the shifted OH band arises from the Fermi resonance between the shifted ν_{OH} and the first overtones of the δ_{OH} and γ_{OH} vibrational modes. The two higher-frequency-shifted OH features (A and B bands at ~2900 and ~2400 cm^{-1}, respectively) are the results of the Fermi resonance between the shifted ν_{OH} and the $2\delta_{OH}$ (in-plane O–H bending) vibrations. The low-frequency IR feature (C band at ~1700 cm^{-1}) can be seen in the spectrum as the result of the Fermi resonance between the shifted ν_{OH} and the $2\gamma_{OH}$ (out-of-plane O–H bending) vibrational modes. The shapes and the intensities of these bands are determined by the strength of the interaction between the protons and the basic molecules. In our study, the "C" component of the broad

IR feature (at ~1700 cm^{-1}) cannot be seen since it is obscured by the other high-intensity vibrational features. It is also possible that this feature is absent in our system because the interaction of the proton and the NO_2 molecule may not be sufficiently strong.

Infrared spectra recorded at reaction times of 0, 5, 10, and 20 min are displayed in Fig. 2A, 1–5. The intensity of the 2133 cm^{-1} feature increases gradually with time while that of the 3615 cm^{-1} band decreases. However, after reacting for 10 min the intensity of these two bands did not change significantly. In contrast, the intensities of the two new features at 1883 and 1574 cm^{-1} continue to gradually increase with time. The addition of a second dose of oxygen to the system resulted in further changes in the IR spectrum. The spectral feature at 2133 cm^{-1} decreases upon addition of the second oxygen dose and at the same time two new IR bands develop at 2185 and 1745 cm^{-1}. The intensities of these bands increase with time just as the two other peaks at 1872 and 1587 cm^{-1} did. The frequencies of these two latter IR features gradually shifted as their intensities increase. The IR band that has a peak position of 1833 cm^{-1} at low concentrations red shifts while that of the 1574 cm^{-1} peak blue-shifts with increasing coverage. At their maximum intensities they are centered at 1872 and 1587 cm^{-1}, respectively. Meanwhile, the intensity of the acidic O-H vibrational band remained unchanged. Introduction of a third aliquot of oxygen did not result in the formation of any new vibration band, although the intensities of the existing features changed. Namely, the intensity of the 2133 cm^{-1} band further decreased, while that of the 2185 cm^{-1} peak increased. The intensities of all the other IR features in the 1400–1900 cm^{-1} region increased further. An isosbestic point at 2149 cm^{-1} can clearly be seen at high oxygen doses, which suggests a direct correlation between the adsorbed surface species responsible for the IR features at 2133 and 2185 cm^{-1}.

Closer inspection of the series of IR spectra of Fig. 2 also reveals that the IR absorption band at 1745 is absent from the spectrum as long as there is only a single, highly symmetric band centered at 2133 cm^{-1} present. As soon as a shoulder develops on the high-frequency side of the 2133 cm^{-1} band, a new IR feature appears at 1745 cm^{-1}. As the intensity of the 2133 cm^{-1} band decreases and it becomes increasingly asymmetric, the 2185 cm^{-1} feature grows in and the intensity of the 1745 cm^{-1} band increases as well. Furthermore, there is a good correlation between the intensities of the 1883–1872 and 1574–1587 cm^{-1} IR features. In Fig. 3, the integrated IR intensity of the 1587 cm^{-1} band is plotted as a function of that of the 1872 cm^{-1} feature. The data points fall on a straight line with a slope of 1.01. Hoost *et al.* (21) assigned the 1587 cm^{-1} band to adsorbed NO_2 (together with features at ~1650 cm^{-1}) on H-ZSM-5. However, no 1872 cm^{-1} band was reported in Ref. (21) either after NO_2 adsorption on H-ZSM-5 or during the $NO + O_2$ reaction on CuH-ZSM-5. These two features may represent adsorbed N_2O_3 species formed in the presence of NO and O_2. The three IR absorption bands observed at 1876, 1578, and 1298 cm^{-1} by Aylor *et al.* (45) in the decomposition of NO over a Cu-ZSM-5 catalyst were attributed to adsorbed N_2O_3 species. The assignment was based on the good agreement between the peak positions observed in Ref. (45) and those reported for solid N_2O_3 (46). The IR band centered at 1745 cm^{-1} has been assigned to adsorbed N_2O_4 (21).

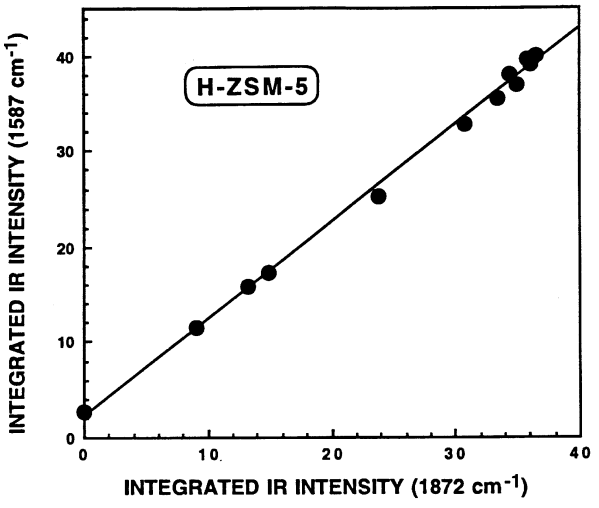

FIG. 3. Correlation between the integrated IR intensities of the 1587 and 1872 cm^{-1} bands over H-ZSM-5 in the $NO + O_2$ reaction at 300 K.

To explain these observations the following model is suggested: Over the H-ZSM-5 zeolite NO does not decompose with appreciable rate under the given reaction conditions. The absence of any significant IR features of the decomposition products or intermediates is good evidence of this assertion. The low-intensity features seen in the IR spectra in the absence of gas-phase oxygen probably originate from the slow disproportionation processes that can take place even over the Na- and H-form zeolites (31, 32). The introduction of a small amount of oxygen results in the formation of NO_2 according to the following equation:

$$NO + 1/2\,O_2 \Leftrightarrow NO_2. \qquad [1]$$

The NO_2 produced, in turn, interacts with the Brønsted acidic hydroxyl groups of the zeolite. The $H^+\cdots NO_2$ adsorption complex is responsible for the IR feature centered at 2133 cm^{-1} (spectrum 2 in Fig. 2) with initially no other bands observed. During the 20 min time interval, the intensity of the 2133 cm^{-1} feature reaches its maximum; additionally, two new IR absorption bands develop at 1883 and 1574 cm^{-1}. These two features arise from the N_2O_3 species formed by the interaction of the *in situ* produced NO_2 and the NO, which is present in large excess in the reaction cell. This assignment explains the linear correlation found for the integrated intensities of these two IR features shown in

Fig. 3. As the concentration of the NO_2 increases the number of N_2O_3 molecules formed by the equilibrium process increases concomitantly:

$$NO_2 + NO \Leftrightarrow N_2O_3. \quad [2]$$

Despite the slight increase in the concentration of NO_2 (evidenced by the intensity gains of the N_2O_3 features), the 2133 cm^{-1} band reaches its maximum intensity after 5 min reaction time. Additionally, the complete disappearance of the acidic OH vibrational feature at 3615 cm^{-1} occurs at this point. Furthermore, the intensity of this latter band remains unchanged upon the introduction of additional oxygen aliquots. Correlating these observations suggests a direct connection between the 2133 and 3615 cm^{-1} features. Formation of NO_2 does not stop at the point in time when the 3615 cm^{-1} band disappears, but rather indicates that all the protons have reacted with NO_2. Therefore, further increase in the concentration of gas-phase NO_2 can not be tracked by following the intensity of either the 2133 or the 3615 cm^{-1} IR feature.

The introduction of the second oxygen aliquot results in the formation of a gradually increasing amount of NO_2. The increased concentration of NO_2 is responsible for the increased production of N_2O_3 by shifting the equilibrium to the right in Eq. [2]. During the 20 min reaction time the intensities of both the 1883 and 1574 cm^{-1} bands sharply increase until they maximize. In addition, two new absorption features develop at 1745 cm^{-1} and as a shoulder on the high frequency side of the 2133 cm^{-1} band (spectra 6–9 in Fig. 2). These features arise from adsorbed N_2O_4 species. The formation of N_2O_4 can not proceed until certain NO_2 and/or N_2O_3 concentrations are achieved. Two possible routes for N_2O_4 formation are (i) dimerization of NO_2,

$$2NO_2 \Leftrightarrow N_2O_4, \quad [3]$$

and (ii) oxidation of N_2O_3 by O_2,

$$N_2O_3 + 1/2\,O_2 \Leftrightarrow N_2O_4. \quad [4]$$

Both equilibrium processes require the presence of NO_2 in high concentration. Introduction of the third oxygen dose shifts the equilibrium of reaction [1] to the right, resulting in the formation of NO_2 in high concentration, which in turn shifts the equilibrium of reaction [3] to the right. The increased NO_2 concentration, brought about by the presence of excess gas-phase oxygen, has the same effect on the N_2O_4 formation through N_2O_3 (reaction [4]). In this scheme, the equilibrium of reaction [2] is shifted to the right by the higher NO_2 concentration and in turn shifts the equilibrium to the right for Eq. [4]. The introduction of the third oxygen aliquot does not change significantly the concentration of N_2O_3 and is indicated by the constant intensities of the 1872 and 1587 cm^{-1} IR bands, while the concentration of N_2O_4 sharply increases resulting in the large intensity gains of both the 1745 and 2185 cm^{-1} features.

Evacuation of the IR cell at 300 K sample temperature for 1 min results in the complete disappearance of the 2185, 1872, 1745, and 1587 cm^{-1} IR bands. Removal of NO and O_2 from the gas phase shifts the equilibria of reactions [1], [2], and [4] toward the left. As the concentration of NO_2 decreases, the equilibrium of reaction [3] shifts to the left as well. These two processes are responsible for the disappearance of the IR features of both the N_2O_3 and N_2O_4 species from the spectrum. The series of IR spectra obtained from the evacuation experiments are shown in Figs. 4A and 4B for the two spectral regions 1400–2350 cm^{-1} (N–O vibrations) and 2400–3800 cm^{-1} (O–H vibrations), respectively. The only remaining IR features are the 2133 cm^{-1} band which gains some intensity upon the 1 min evacuation and a weak band at ~1655 cm^{-1} which might correspond to a nitrate species bound to very low concentration of Na^+ ion residues remaining after the NH_4^+ ion exchange. The intensity of the latter feature does not change upon prolonged evacuation, while that of the 2133 cm^{-1} band decreases slightly during an additional 10 min evacuation but thereafter remains essentially unchanged upon further pumping. Upon desorption of all N_2O_4 and a fraction of NO_2 from the system a large fraction of the bridging Brønsted acidic OH groups reappear at 3615 cm^{-1}. Concomitantly, the very broad IR features centered at ~2485 and ~2905 cm^{-1} originating from the strong H-bonding interaction between the adsorbates and the strongly acidic bridging hydroxyl groups lose substantial intensities upon evacuation. These observations suggest that NO_2 adsorbs strongly onto the protons of acidic bridging hydroxyl groups and that explains why they retain a large portion of their intensity at 2133 cm^{-1} even after prolonged evacuation. The very fast disappearance of the IR features originating from adsorbed N_2O_3 and N_2O_4 suggests that these species are weakly held, although strongly interacting with the Brønsted sites and decompose upon evacuation leaving adsorbed NO_2 behind.

NaH-ZSM-5

An IR spectral series obtained from NaH-ZSM-5 in the presence of 2.8 Torr NO at 300 K in a 0–60 min time interval is shown in Fig. 5A (spectra labeled 1–7 in the spectral region 1400–2350 cm^{-1}). At zero reaction time, the most intense IR feature is the one originating from the gas-phase NO centered at 1876 cm^{-1}. The other bands are the same seen for the H-ZSM-5 sample at initial reaction time. At 300 K, no significant changes are seen in any of the IR bands except for the one at 1637 cm^{-1}. This feature continuously increases with reaction time, and after 60 min it is the most intense absorption band. This feature is suggested to arise from a nitrate species bound onto Na^+ ions in cationic positions. The intensity of the 2126 cm^{-1} feature increases very little with time while the 2252 cm^{-1} band remains constant.

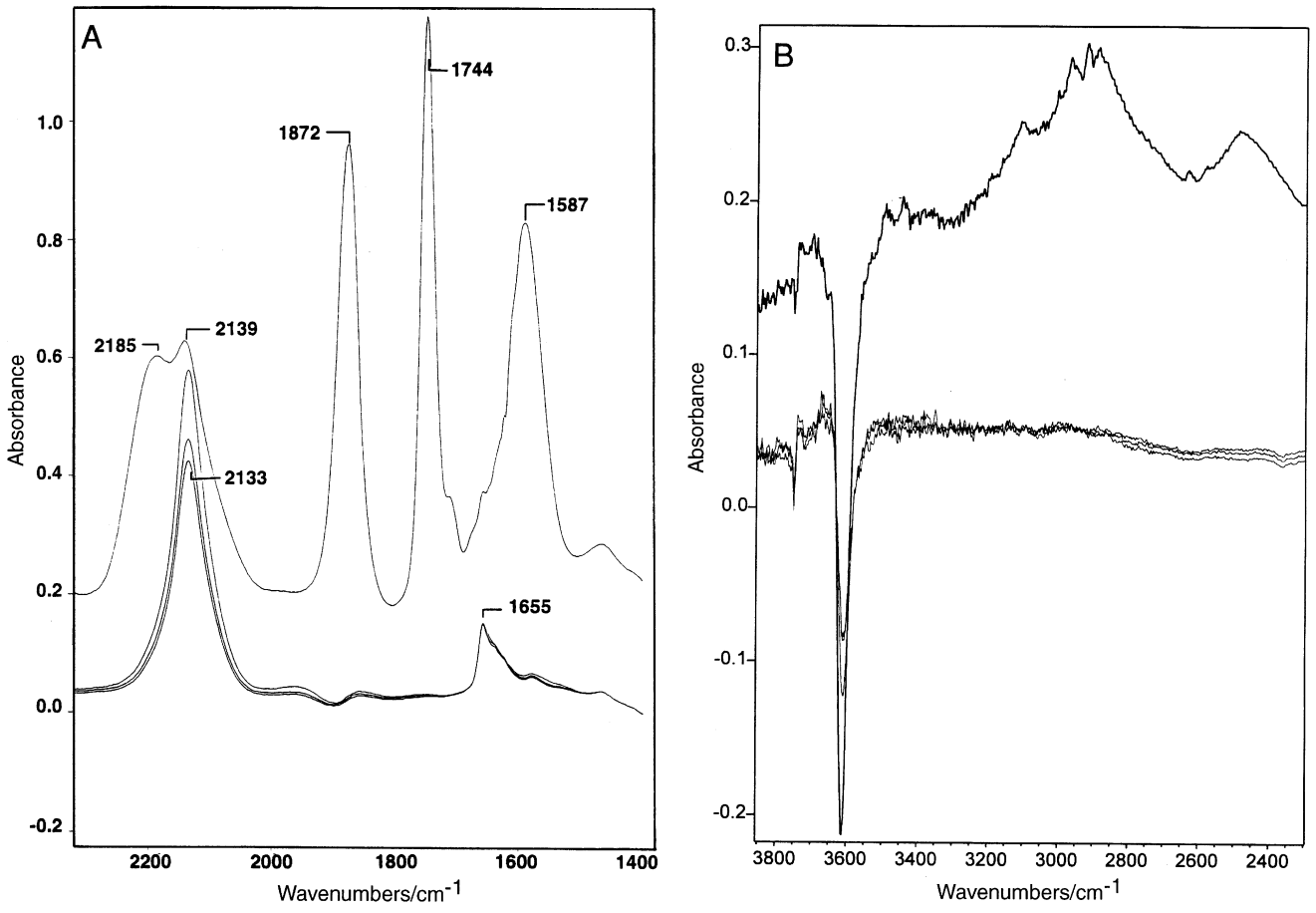

FIG. 4. IR spectra collected from H-ZSM-5 after the completion of the $NO + O_2$ reaction at 300 K (top spectrum) and then following subsequent evacuation at 300 K in the 1400–2350 cm^{-1} (A) and 2400–3800 cm^{-1} (B) regions. Evacuation times: 1 : 00 min (2), 6 : 00 min (3), and 16 : 00 min (4).

These features most probably originate from the interaction between the products of the slow NO disproportionation reaction and the H^+ and Na^+ sites of the zeolite catalyst (31, 32). Introduction of the first dose of oxygen dramatically increases the intensity of the 2133 cm^{-1} feature at the instant of O_2 introduction and produces new IR absorption bands at 1890, 1771, 1555, and 1410–1430 cm^{-1}. Simultaneously the IR bands at 2252 and 1810 cm^{-1} almost completely disappear, while the intensity of the 1638 cm^{-1} feature increases significantly. Allowing the sample to stay in the $NO + O_2$ reaction gas mixture for 20 min results in further growth of the 2133, 1885, 1638, and 1576 cm^{-1} bands, while the low-intensity feature at 1771 cm^{-1} remains constant. After the 20 min reaction time, the 2133 cm^{-1} band reaches its maximum intensity and does not grow further even after the introduction of additional oxygen doses. Two subsequent O_2 doses and 20 min reaction after each O_2 dose did not result in any significant further changes in the IR spectra. The features at 1883, 1635, 1577, and 1415–1430 cm^{-1} become gradually more intense with only a very small increase in the intensity of the 2133 cm^{-1} band. The only new feature in the IR spectrum develops after the last O_2 dose and is centered at 1750 cm^{-1}. The appearance of this IR band correlates with the development of a high-frequency shoulder on the 2133 cm^{-1} band, and with the very slow intensity decrease of this peak. This phenomenon is exactly the same as that discussed previously for the $(NO + O_2)$/H-ZSM-5 system. The more complicated structure of the IR spectra in the 1400–1700 cm^{-1} spectral region observed for the NaH-ZSM-5 as compared with the H-ZSM-5 sample arises from the formation of adsorbed N- and O-containing surface species on both Na^+ and H^+ ions. The 1577 cm^{-1} IR absorption feature together with the 1883 cm^{-1} band represents adsorbed N_2O_3 bound to protonic sites. The peak position of the 1883 cm^{-1} band at the conclusion of the experiment is exactly the same, as we have shown for the H-ZSM-5 sample at identical integrated intensities. The peak position of the 1577 cm^{-1} feature is slightly different from the one we have seen for H-ZSM-5 and is expected because of the overlap between this IR band and the ones originating from the Na^+-bound nitrate species. The intensities of these nitrate features are much higher than those observed for H-ZSM-5 since the concentration of Na^+ ions is much higher in this sample. The H-ZSM-5 sample contained only

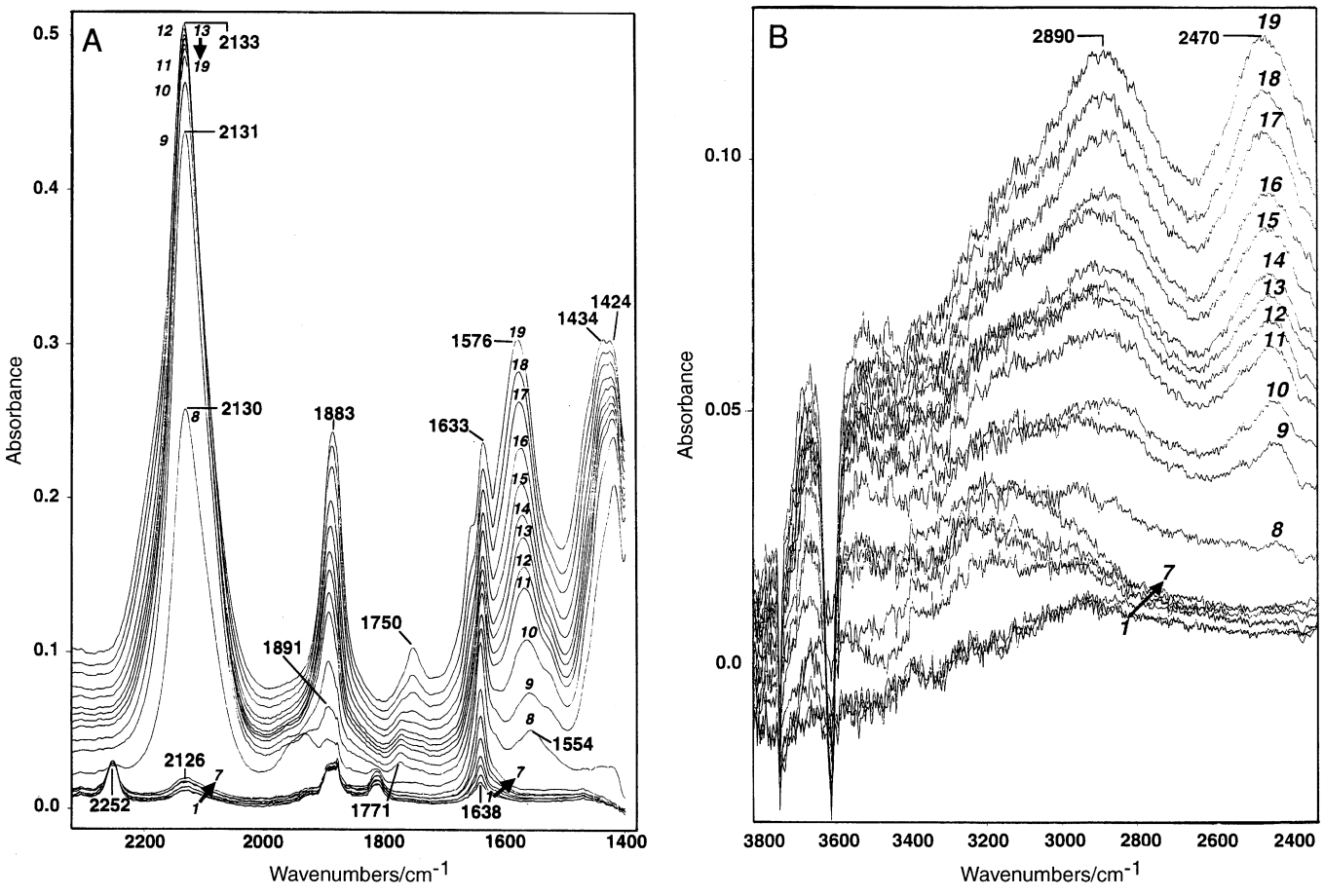

FIG. 5. IR spectra acquired during the NO decomposition and NO + O_2 reaction over NaH-ZSM-5 in the 1400–2350 cm^{-1} (A) and 2400–3800 cm^{-1} (B) regions. Spectra 1–7: NO decomposition (0, 5, 10, 20, 30, 45, and 60 min); 8–11: 7 + first oxygen dose ($P_{O_2} = 0.16$ Torr) (0, 5, 10, and 20 min); 12–15: 11 + second oxygen dose ($P_{O_2} = 0.18$ Torr) (0, 5, 10, and 20 min); 16–19: 15 + third oxygen dose ($P_{O_2} = 0.92$ Torr) (0, 5, 10, and 20 min) [$T = 300$ K; $P_{NO(initial)} = 2.79$ Torr].

a small amount of residual Na^+ ions that remained in the sample after the NH_4^+ ion exchange procedure (Na/Al = 0.004).

It is also informative to follow the changes that occur in the 2300–3800 cm^{-1} spectral region upon NO adsorption and also during the NO + O_2 reaction over NaH-ZSM-5. The series of IR spectra in the 2400–3800 cm^{-1} region corresponding to those shown in Fig. 5A are displayed in Fig. 5B. In the time interval of 0–60 min that the sample spent in the NO atmosphere there is only a very small decrease in the intensity of the 3615 cm^{-1} band and also only a broad, very weak feature developing between 2900 and 3300 cm^{-1}. The introduction of oxygen results in the gradual appearance and increase of both the ~2470 and ~2980 cm^{-1} features. As the 2133 cm^{-1} band reaches its maximum intensity, both of these broad features reach their maximum intensities while the 3615 cm^{-1} band completely disappears. Again, there is a good correlation between the 2133 cm^{-1} feature and the two broad features at higher frequencies (2470 and 2980 cm^{-1}) indicative of basic adsorbates interacting with Brønsted acid OH groups. The intensities of these broad OH features in Na,H-ZSM-5 are naturally lower than those previously seen for the H-ZSM-5 sample because the number of acidic OH groups is obviously much lower than that in H-ZSM-5.

The chemistry seen for the (NO + O_2)/Na,H-ZSM-5 system is nearly identical to that previously discussed for the H-ZSM-5 catalyst. In the IR spectra, the same adsorbed species are observed with the differences being the much higher intensities of IR bands representing Na^+ bound N_xO_y species on this sample compared to the H-ZSM-5. This is a direct and obvious consequence of the high Na^+ concentration in this catalyst.

Evacuation of the system following the NO + O_2 reaction results in the disappearance of all the IR absorption features originating from adsorbed N_2O_3 and N_2O_4 species. The only remaining IR bands are the ones which arise from (a) adsorbed NO_2 species on protons (2133 cm^{-1}), and (b) nitrites and nitrates associated with Na^+ ions (1420,

1638, and 1654 cm^{-1}). Concomitant to the disappearance of the N_2O_3 and N_2O_4 bands and the decrease in NO_2 concentration, the shifted OH vibrational features lose large portions of their intensities, paralleled by the reappearance of the 3615 cm^{-1} feature of the adsorbate free bridging hydroxyls.

CuH-ZSM-5

The adsorption of NO on CuH-ZSM-5 produces the same IR features as have been reported for the NO/Cu-ZSM-5 systems by several research groups (2, 3, 21, 44). The main features present in the IR spectrum collected at reaction time equal to zero are the ones that correspond to NO adsorbed on both Cu^+ and Cu^{2+} sites. Specifically, the two features at 1734 and 1823 cm^{-1} arise from the respective asymmetric and symmetric NO-stretching vibrations of dinitrosyl species at Cu^+ sites. The 1811 cm^{-1} band represents mononitrosyl species bound to Cu^+ sites. Also, there is a fairly intense vibrational feature centered at 1908 cm^{-1} which has been assigned to NO adsorbed onto Cu^{2+} ions located in cationic positions of the ZSM-5 structure. The decomposition of NO was followed at an initial NO pressure of 10.1 Torr for 60 min and IR spectra were collected at several reaction times. The IR spectra series collected during the decomposition of NO over CuH-ZSM-5 at 300 K is shown in Fig. 6. It is evident from the IR spectra obtained that the decomposition of NO proceeds more rapidly on the CuH-ZSM-5 catalyst than over either the H- or NaH-ZSM-5 sample. The concentration of the Cu^+ bound dinitrosyl species gradually decreases with reaction time and is indicated by the continuous decrease in the intensities of the 1823 and 1734 cm^{-1} bands. Meanwhile, the intensity of the 1908 and 2135 cm^{-1} features increase rapidly with time as a result of (a) an increase in the number of Cu^{2+} sites available for NO adsorption due to the oxidation of Cu^+ sites by NO and (b) the production of NO_2 species during the NO decomposition which then adsorb at residual protonic sites, respectively. Associated with the gradual intensity increase of these two features are concomitant small spectral shifts from 1908 to 1910 cm^{-1} and from 2135 to 2133 cm^{-1} in these respective band positions. Parallel to the increase in the intensity of the 2133 cm^{-1} band there is a decrease in the intensity of the 3615 cm^{-1} feature, corresponding to an interaction with residual acidic OH groups. The integrated IR intensities of the 2133, 1910 and 3515 cm^{-1} features are plotted in Fig. 7 as a function of reaction time. The correspondence between the increase in the intensity of the 2133 cm^{-1} feature and the consequent decrease in the intensity of the 3615 cm^{-1} band is clearly evident from this figure, while the intensity of the 1910 cm^{-1} peak increases monotonically with reaction time. Again, there is an excellent, direct correlation between the acidic OH groups and the adsorbed NO_2 species responsible for the 2133 cm^{-1} band. With increasing reaction

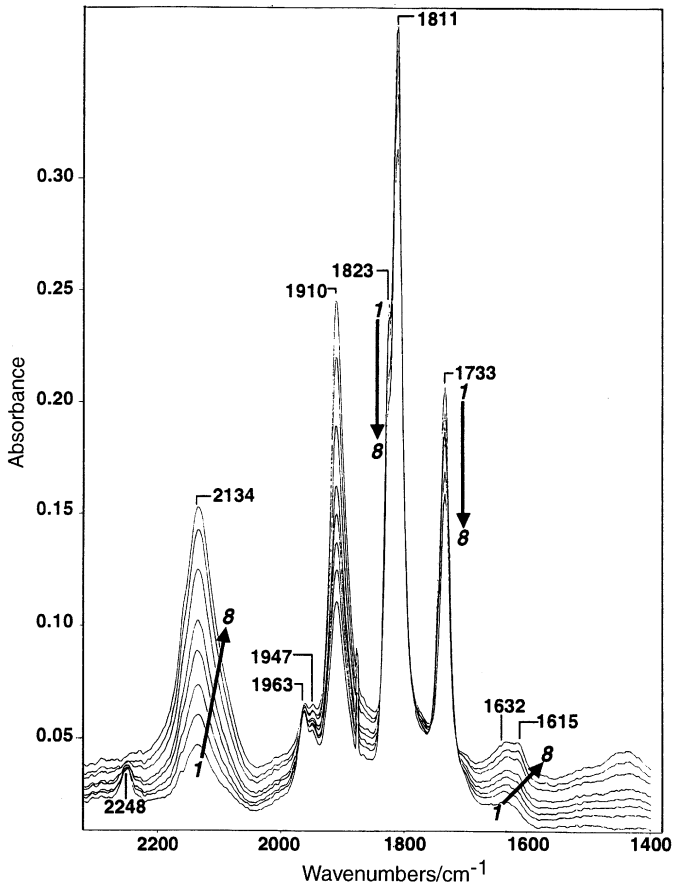

FIG. 6. IR spectra obtained from CuH-ZSM-5 in the presence of NO. Spectra (1–8) were collected at 0, 5, 10, 15, 20, 30, 45, and 60 min [$T = 300$ K; $P_{NO(initial)} = 10.14$ Torr].

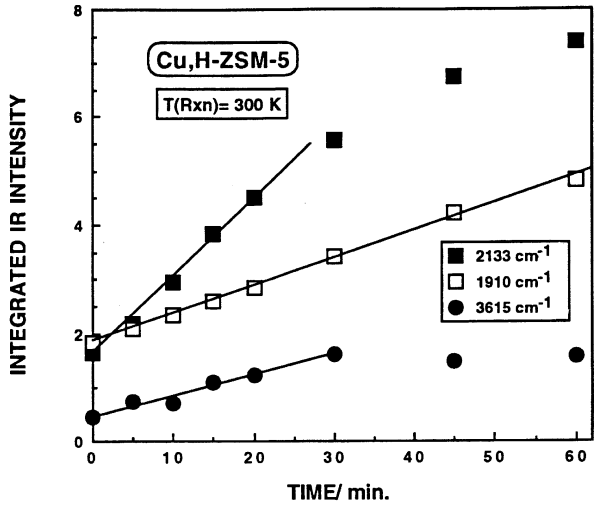

FIG. 7. Integrated IR intensities of the 2133, 1910, and 3615 cm^{-1} bands as a function of reaction time during NO decomposition over CuH-ZSM-5 [$T = 300$ K; $P_{NO(initial)} = 10.14$ Torr]. (Negative intensities for the 3615 cm^{-1} feature are shown.)

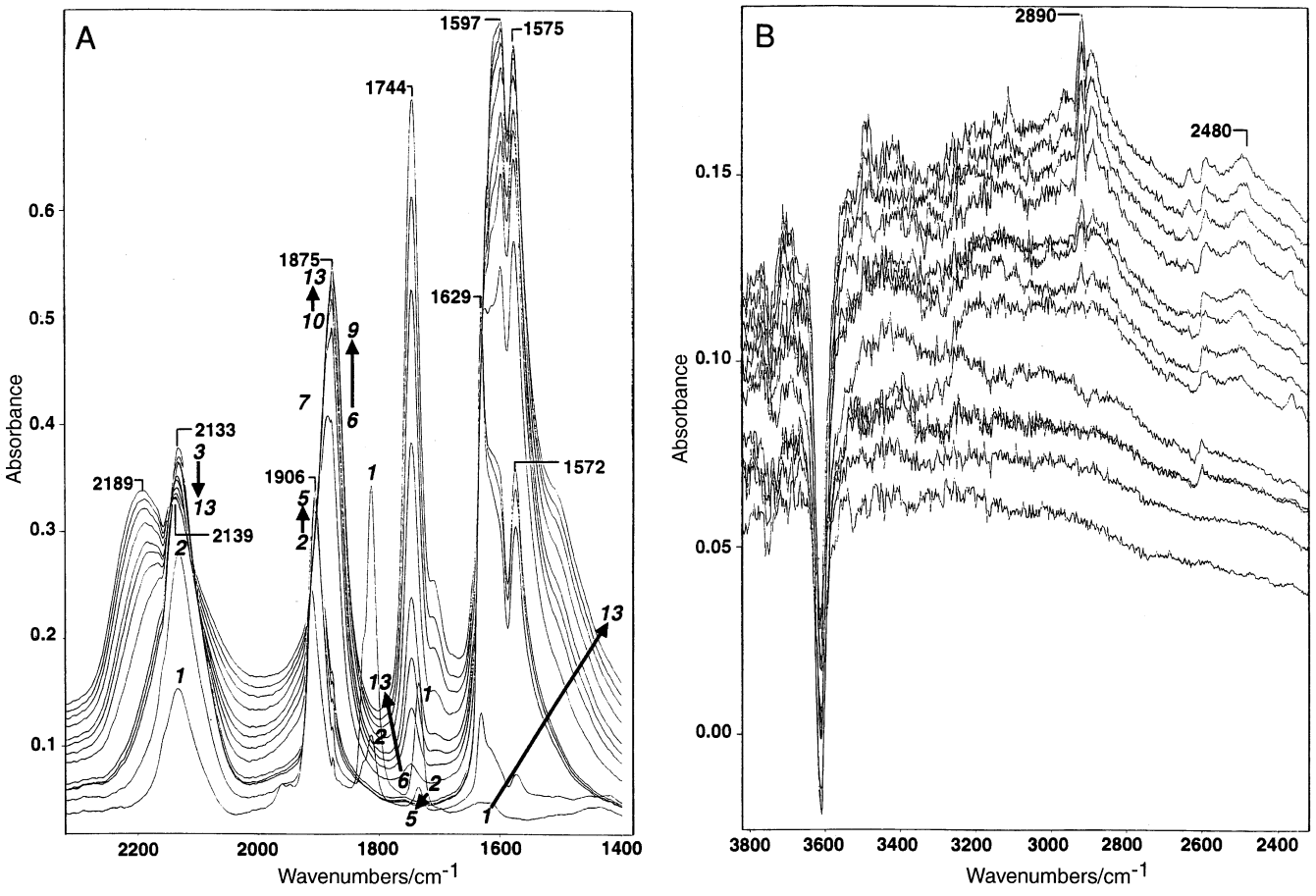

FIG. 8. IR spectra obtained from CuH-ZSM-5 during the NO + O_2 reaction in the 1400–2350 cm^{-1} (A) and 2400–3800 cm^{-1} (B) regions. Spectra 1: after 60 min NO decomposition at 300 K (spectrum 8 in Fig. 6); 2–5: 1 + first dose of oxygen ($P_{O_2} = 0.53$ Torr) (0, 5, 10, and 20 min); 6–9: 5 + second dose of oxygen ($P_{O_2} = 1.31$ Torr) (0, 5, 10, and 20 min); 10–13: 9 + third dose of oxygen ($P_{O_2} = 2.15$ Torr) (0, 5, 10, and 20 min) [$T = 300$ K; $P_{NO(initial)} = 10.14$ Torr].

time, the appearance and subsequent growth of two new features at 1614 and 1632 cm^{-1} can also be seen in Fig. 6. These bands have been assigned to adsorbed NO_2^- and surface nitrate (21) species, respectively, formed during the decomposition of NO over CuH-ZSM-5.

As seen previously for the H- and NaH-ZSM-5 samples, the introduction of the first small oxygen dose results in significant changes in the IR spectra of CuH-ZSM-5 (Figs. 8A and 8B). The intensities of the Cu^+-bound NO species (both mono- and dinitrosyl) drop to zero almost instantaneously upon the introduction of O_2. Meanwhile, the intensities of the 2133 and 1910 cm^{-1} bands increase dramatically and there are also large increases in the intensities of the bands located in the 1500–1650 cm^{-1} region. After 20 min reaction time in the NO + O_2 gas mixture, the 2133 and 1910 cm^{-1} features reach their maximum intensities and no trace of NO species adsorbed on Cu^+ is observed. The introduction of the second aliquot of oxygen brings about further changes in the IR spectrum. A noticeable shoulder on the high frequency side of the 2133 cm^{-1} band appears and gradually increases with time. Simultaneously, a new IR feature grows in at 1745 cm^{-1} and its intensity increases rapidly with time. Furthermore, the 1910 cm^{-1} band shifts to 1875 cm^{-1} and its intensity increases. The intensities of the features in the 1500–1650 cm^{-1} range also increase significantly. The addition of the third dose of oxygen results in the decrease of the 2133 cm^{-1} and the concomitant growth of both the 2185 and 1745 cm^{-1} bands. The intensity of the 1875 cm^{-1} peak saturates and does not change during the 20 min reaction time.

The 2400–3800 cm^{-1} spectral region is shown in Fig. 8B in which the spectra correspond to those displayed in Fig. 8A. The intensities of all the IR features are significantly lower than those reported for both the H- and NaH-ZSM-5 catalysts. This observation suggests the obvious in that the concentration of the protonic sites in the Cu,H-ZSM-5 sample is significantly lower than in the two other catalysts discussed previously. However, even at this low proton concentration the presence of the two associated, shifted hydroxyl bands can clearly be seen at ~2480 and ~2890 cm^{-1}.

They reach their maximum intensities as the signature of the acidic OH groups at 3615 cm^{-1} disappears (maximum negative intensity at 3615 cm^{-1}).

The interpretation of the IR spectra obtained in the $NO + O_2$ gas mixture follows several general trends. In the presence of oxygen NO rapidly oxidizes to NO_2 resulting in the rapid concentration increase of proton-bound NO_2 surface species. This is indicated by the rapid growth of the 2133 cm^{-1} band. Simultaneously, the number of Cu^{2+} sites increases due both to the presence of gas-phase oxygen and the NO decomposition reaction. As the concentration of these Cu^{2+} sites increases the intensity of the 1910 cm^{-1} feature increases. In addition, there are increases in the concentration of other adsorbed NO_x species in this oxygen rich environment producing intense absorption features in the 1500–1650 cm^{-1} spectral region. As the concentration of the NO_2 entities produced by the $NO + O_2$ reaction increases the number of proton-bound NO_2 species increases as well. As the available protonic acid sites are consumed by the adsorption of NO_2, the 2133 cm^{-1} band reaches its maximum intensity concomitant with no further decrease in the intensity of the 3615 cm^{-1} OH-stretching vibration. As soon as the NO_2 concentration reaches a critical concentration the special features attributed to adsorbed N_2O_4 species develop (vibrational features at 2185 and 1745 cm^{-1}). Nitrogen dioxide (N_2O_4) can form by the same two reaction pathways we have discussed in detail for the H-ZSM-5 catalyst, either through N_2O_3 or by the dimerization of NO_2, and probably both. Regardless of the reaction route that produces N_2O_4, it requires the presence of a critical concentration of NO_2 in the reaction system. The intensities of these two bands increase rapidly as N_2O_4 forms. At high oxygen doses, the formation of Cu coordinated to oxygen is evident from the IR spectra. The result of this oxidation step is the development of the 1875 cm^{-1} band which corresponds to the vibrations of NO molecules adsorbed onto CuO. This feature is observed at exactly the same frequency as observed for NO adsorption on an alumina supported CuO catalyst (21). In this system, however, this feature is a composite of two closely spaced IR absorption bands. One feature arises from the *in situ* formed N_2O_3 adsorbed onto the Brønsted acidic bridging hydroxyl groups, while the other band represents NO molecules adsorbed onto CuO entities. The very close proximity of these two IR bands makes it impossible to separate these two features. However, the changing band shape as the CuO···NO adsorption complex develops is consistent with the suggestion that this feature is indeed the superposition of two individual absorption bands.

Following the NO decomposition and $NO + O_2$ reaction over Cu,H-ZSM-5, the evacuation of the IR cell for 10 min at 300 K sample temperature results in the disappearance of all the absorption features originating from weakly adsorbed N_xO_y surface species. The IR adsorption features of adsorbed N_2O_3 (1875 and 1587 cm^{-1}) and N_2O_4 (2185 and 1745 cm^{-1}) are completely eliminated by this brief evacuation while the IR signatures of strongly adsorbed N_xO_y entities remain. The intensity of the 2133 cm^{-1} band (H^+ adsorbed NO_2) increases somewhat and that of the 1500–1650 cm^{-1} features decrease significantly due mainly to the loss of the 1587 cm^{-1} band of adsorbed N_2O_3.

Cu-ZSM-5

The last catalyst investigated in the adsorption and decomposition of NO and the $NO + O_2$ reaction was a solid-state ion exchanged Cu-ZSM-5. This sample was prepared in order to study the NO decomposition and the $NO + O_2$ reaction on a Cu-ZSM-5 catalyst which contained no measurable amount of protonic acid sites by IR spectroscopy. The IR spectrum of the adsorbate free solid state ion exchanged Cu-ZSM-5 catalyst revealed that no Brønsted acidic OH groups survived the solid-state ion exchange with CuCl vapor and the subsequent annealing, as was evidenced by the complete absence of the 3615 cm^{-1} OH vibrational signature. The large decrease in the intensity of the high frequency OH band suggested that a significant portion (>50%) of the terminal silanol OH groups have also reacted with the CuCl vapor providing additional adsorption/reaction sites. The presence of these additional Cu species was indicated from low temperature CO adsorption experiments. Infrared measurements of CO adsorption at 150 K $< T_{ads.} <$ 300 K strongly suggested that no metallic copper or copper-oxide particles formed on the outer surface of the catalyst or in the pores of the zeolite. Infrared spectra collected following room temperature CO adsorption display only one highly symmetrical absorption feature centered at 2157 cm^{-1} at low and moderate CO pressures. This feature has been regarded as a good signature for the presence of isolated Cu^+ adsorption sites located in cationic positions in the ZSM-5 structure (22). At higher CO pressures, several IR features that can be assigned to di- and tricarbonyl surface species on Cu^+sites in solid-state ion exchanged Cu-ZSM-5 materials are seen (22). The decomposition of NO at 300 K at an initial NO pressure of 10.2 Torr was followed for 2 h. IR spectra were collected at several reaction times and are displayed in Fig. 9 as a spectral series (spectra 1–10). The spectral features are very similar to those shown previously for Cu,H-ZSM-5 in Fig. 6, although some important differences are apparent. At the beginning of the NO decomposition reaction, IR features corresponding to the vibrations of mono- (1811 cm^{-1}) and dinitrosyl (1733 and 1823 cm^{-1}) species adsorbed on Cu^+ sites and a weak Cu^{2+}-bound NO entity (1894 cm^{-1}) are initially seen. A weak IR feature was also seen at 2158 cm^{-1} which is suggested (45) to originate from Cu^+-adsorbed N_2 molecules formed in the decomposition of NO over this catalyst. The intensities of the Cu^+-bound NO species (both mono- and dinitrosyl) gradually decrease with reaction time, while that

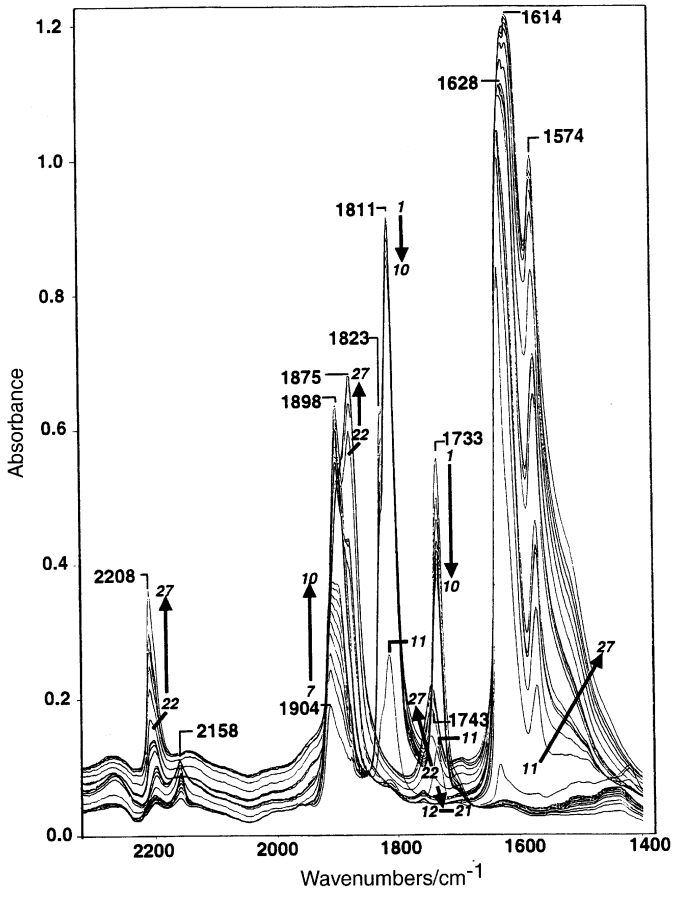

FIG. 9. IR spectra collected during NO decomposition and NO + O_2 reaction on Cu-ZSM-5. Spectra 1–10: NO decomposition (0, 5, 10, 20, 30, 45, 60, 80, 100, and 120 min); 11–16: 10 + first oxygen dose ($P_{O_2} = 0.54$ Torr) (0, 5, 10, 20, 30, and 40 min); 17–21: 16 + second oxygen dose ($P_{O_2} = 0.55$ Torr) (0, 8, 15, 20, and 30 min); 22–27: 21 + third oxygen dose ($P_{O_2} = 1.43$ Torr) (0, 5, 10, 15, 20, and 40 min) [$T = 300$ K; $P_{NO(initial)} = 10.19$ Torr].

of the Cu^{2+}-adsorbed NO increases as a result of the increase in the number of Cu^{+} sites arising from the oxidation process that takes place during NO decomposition. Note that the Cu^{2+}–NO feature broadens as the reaction progresses, and at longer reaction times the presence of two different adsorbed species can be seen. This can be interpreted as either the adsorption of NO at two distinct Cu^{2+} sites having slightly differing crystallographic cation positions or as the adsorption of NO on distinct Cu^{2+} sites located at both cationic positions and those associated with terminal silanol groups. Recently published results of a combined photoluminescence, IR and EPR study (44) on several Cu ion exchanged zeolites revealed that a number of Cu cationic positions exist in these materials. The IR spectra of adsorbed NO on Cu^{2+} in Cu-ZSM-5 zeolites in Ref. (44) show absorption bands at frequencies very close to the ones seen on our samples. These Cu^{2+} sites were shown to differ from each other in their coordination geometries. The Cu^{2+} ions that produce the IR band at ~1910 cm^{-1} upon NO adsorption have square pyramidal geometry, while the 1895 cm^{-1} band has been attributed to square planar coordination (44). The NO adsorption/decomposition experiments described herein indicate that upon NO decomposition those Cu^{+} ions initially involved are oxidized to Cu^{2+} species of square-pyramidal coordination geometry. Those sites that produce Cu^{2+} in the square planar geometries are more stable and require a longer time interval for their creation. The more intense 1895 cm^{-1} feature relative to the 1910 cm^{-1} band in Ref. (44) was suggested to arise from the high Cu loading in these zeolites. This is in good agreement with our observations. For the Cu-acetate solution exchanged CuH-ZSM-5 sample upon NO adsorption/decomposition only one Cu^{2+}-NO_a band at 1910 cm^{-1} is observed (see Fig. 6), while on the solid-state ion exchanged (high Cu exchange level) two Cu^{2+} sites with different NO adsorption properties can be distinguished (note the two distinct $Cu^{2+}\cdots NO_a$ absorption features in Fig. 9).

The most striking characteristic of these IR spectra is the complete absence of the 2133 cm^{-1} absorption band. There are two possible explanations for this. The simplest argument assumes that since this feature is absent in the spectrum the catalyst does not produce NO_2 molecules that account for the 2133 cm^{-1} band. This explanation, however, can be dismissed on the basis of two observations. First, in the 1400–1650 cm^{-1} spectral region absorption features originating from the vibrations of adsorbed, oxidized adsorbed NO_x species can clearly be seen (surface nitrates, nitrites, etc.). Chemical intuition and the results of adsorption experiments carried out with NO_2 have unequivocally demonstrated that the formation of these surface species requires the presence of NO_2 in the system. Furthermore, this and other studies (21, 42) have demonstrated that Cu,H-ZSM-5 is active in the formation of adsorbed NO_2 species, while both the H- and Na,H-ZSM-5 catalysts were inactive for this reaction in the absence of gas-phase oxygen. These observations conclusively support the assumption that Cu^{+} centers are the active sites for the formation of NO_2 in the decomposition of NO, while the Na^{+} and H^{+} ions are inactive in this reaction. From these facts we conclude that the solid state ion exchanged Cu-ZSM-5 does produce NO_2; therefore, the absence of the 2133 cm^{-1} band must be the consequence of the absence of the adsorption sites responsible for the formation of the surface species giving rise to this IR feature (Brønsted acid bridging hydroxyl groups).

The addition of the first oxygen aliquot to the NO/Cu-ZSM-5 system results in the rapid disappearance of the IR bands originating from the Cu^{+}-adsorbed surface NO species. The IR signatures of both the mono- and dinitrosyl adsorbed on Cu^{+} sites rapidly decrease and subsequently disappear after 5 min reaction time. Concomitantly, the IR signatures of the Cu^{2+}-bound NO and the nitrate and nitrite species in the 1400–1650 cm^{-1} spectral

region increase dramatically immediately after the introduction of the oxygen dose. After 10 min reaction time, these features gain further intensity although at a much decreased rate. There are no new features observable in the spectra above 2000 cm^{-1}. As the intensity of the 1904 cm^{-1} band increases (NO adsorbed on Cu^{2+}), its peak position gradually shifts toward lower wavenumbers. The introduction of a second oxygen dose results in a further intensity gain of the 1898 cm^{-1} band and features in the 1400–1650 cm^{-1} spectral region. With increasing reaction time, a shoulder on the low-frequency side of the 1898 cm^{-1} band develops and gradually gains intensity. The introduction of the third oxygen dose results in the full development of a band at 1875 cm^{-1} at the expense of the feature at 1898 cm^{-1}. There is still no IR feature at 2133 cm^{-1}, but two new low-intensity features show up at 2208 and 1743 cm^{-1}. Their intensities remain low even after 40 min reaction time.

For the $NO + O_2$ reaction on Cu-ZSM-5, the most intense absorption bands are the ones which represent adsorbed species on Cu^{2+} sites. During NO decomposition and following the first O_2 dose the intensity of the 1902 cm^{-1} feature (NO adsorbed on Cu^{2+}) and the concentration of the nitrate and nitrite species increase very fast. In the presence of a large amount of oxygen the 1875 cm^{-1} band is extremely intense. This feature corresponds to NO adsorbed at CuO sites. This observation is not surprising since in the Cu-ZSM-5 sample the concentration of Cu ions is very high and under strongly oxidizing conditions the formation of CuO species is expected. The interconversion of the 1898 cm^{-1} band into the 1875 cm^{-1} feature suggests that the CuO entities are not CuO particles outside the zeolite framework or in the channels but rather copper ions in cationic positions becoming progressively oxidized. The appearance and then parallel development of the 1743 and 2208 cm^{-1} bands under highly oxidizing conditions may be explained by one of two possibilities. These features may correspond to the same adsorbed N_2O_4 entities discussed previously for the proton containing catalyst. Under strongly oxidizing conditions, CuO particles may form which can result in the removal of copper ions from cationic positions. The resulting cation sites then would be populated by protons which originate from trace water always present in the system. The complete absence of even traces of the bridging hydroxyl groups at 3615 cm^{-1} or the shifted associated OH features due to interaction with N_xO_y species suggests that the 1743 and 2208 cm^{-1} bands are not the same as those observed for the proton containing materials. Note that the 2208 cm^{-1} band is much narrower than the 2185 cm^{-1} feature on the other samples. The other possible origin of these two features is that they correspond to N_2O_4 species; however, they adsorb to sites other than protons. This assertion is supported by the slightly different positions of both spectral features than previously seen for N_2O_4 adsorbed on the protonic sites. At present, we cannot conclusively assign these IR bands on the basis of our experimental data; however, *ab initio* calculations are underway to provide guidance to the possible band assignments.

Evacuation of the IR cell for 15 min at 300 K following the decomposition of NO and the $NO + O_2$ reaction over Cu-ZSM-5 results in the complete disappearance of the features located between 1870 and 1900 cm^{-1} and the large intensity drop of the 1743 cm^{-1} band as well. In contrast, no decrease in the intensities of the 2208 cm^{-1} band and the features between 1500 and 1650 cm^{-1} are observed. These low-frequency features represent strongly adsorbed N_xO_y species bound to copper sites. The same features were seen for the Cu,H-ZSM-5 sample, although on that sample the intensities decreased upon evacuation, while for the Cu-ZSM-5 sample no decrease is seen. This can be explained by the absence of the proton-bound N_2O_3 species on the Cu-ZSM-5 sample, while on the Cu,H-ZSM-5 catalyst this species is present, giving an intense IR band at 1587 cm^{-1} which overlaps with the copper-bound strongly held N_xO_y entities.

CONCLUSIONS

In situ measurements of H-, NaH-, CuH-, and Cu-ZSM-5 in the presence of NO and O_2 are summarized by the following conclusions:

(i) *In situ* IR measurements of NO decomposition have confirmed previous results demonstrating that Cu loaded ZSM-5 (ion or solid-state exchange) is intrinsically much more reactive than H- or NaH forms of ZSM-5.

(ii) The role of Brønsted acid protons has been shown to nucleate N_xO_y species in H-ZSM-5, NaH-ZSM-5, and CuH-ZSM-5 zeolites in the presence of NO and O_2.

(iii) Time evolution of the IR signatures for N_xO_y species produced after controlled oxygen exposure demonstrate a strong correlation among N_2O_3 and N_2O_4 adsorbed species. Equilibrium reactions in which adsorbed NO_2 and O_2 react to produce N_2O_3 and which then further reacts with O_2 to create N_2O_4 are postulated to account for these spectral observations.

(iv) The interaction of the *in situ* formed N_2O_3 and N_2O_4 with Brønsted acid protons is sufficiently strong that the O–H stretch exhibits a classical "ABC" type Fermi resonant structure. The N_2O_3 and N_2O_4 adsorbed species, are, however, only weakly adsorbed and rapidly disappear upon evacuation. Adsorbed NO_2 at proton sites and nitrite and nitrate species are stable to evacuation.

(v) Copper in the zeolite host exhibits reactivity patterns initiating from a mixed mononitrosyl and dinitrosyl species. Oxygen rapidly consumes Cu adsorbed NO to produce adsorbed NO_2 and nitrites and nitrates. Partial oxidation of Cu sites to Cu^{+2} is also seen.

ACKNOWLEDGMENTS

We thank Pam Gordon for the preparation of the H-, NaH-, and CuH-ZSM-5 samples. We also thank the Science and Technology Base Office of LANL for support of portions of this work.

REFERENCES

1. Iwamoto, M., *in* "Zeolites and Related Microporous Materials: State of the Art 1994" (J. Weitkamp *et al*., Eds.). Studies in Surface Science and Catalysis, Vol. 84, p. 1395. Elsevier, Amsterdam, 1994.
2. Iwamoto, M., Mizuno, N., and Yahiro, H., *in* "Proceedings, 10th International Congress on Catalysis, Budapest, 1992" (L. Guczi, F. Solymosi, and P. Tetenyi, Eds.), p. 1287. Elsevier, Amsterdam, 1993.
3. Valyon, J., and Hall, W. K. *in* "Proceedings, 10th International Congress on Catalysis, Budapest, 1992" (L. Guczi, F. Solymosi, and P. Tetenyi, Eds.), p. 1339. Elsevier, Amsterdam, 1993.
4. Shelef, M., Montreuil, C. N., and Jen, H. W., *Catal. Lett.* **26**, 277 (1994).
5. Jen, H. W., and Otto, K., *Catal. Lett.* **26**, 217 (1994).
6. Li, Y., and Hall, W. K., *J. Phys. Chem*. **94**(16), 6145 (1990).
7. Hall, W. K., and Valyon, J., *Catal. Lett.* **15**, 311 (1992).
8. Giamello, E., Murphy, D., Magnacca, G., Morterra, C., Shioya, Y., Nomaru, T., and Anpo, M., *J. Catal.* **136**, 510 (1992).
9. Petunchi, J. O., and Hall, W. K., *Appl. Catal. B: Environmental* **2**, L17 (1993).
10. Li, Y., and Hall, W. K., *J. Catal.* **129**, 202 (1991).
11. Valyon, J., Millman, W. S., and Hall, W. K., *Catal. Lett.* **24**, 215 (1994).
12. Ishihara, T., Kagawa, M., Hamada, F., and Takita, Y., *in* "Zeolites and Related Microporous Materials: State of the Art 1994" (J. Weitkamp *et al*., Eds.). Studies in Surface Science and Catalysis, Vol. 84, p. 1493. Elsevier, Amsterdam, 1994.
13. Moretti, G., *Catal. Lett.* **23**, 135 (1994).
14. Campa, M. C., Indovina, V., Minelli, G., Moretti, G., Pettiti, I., Porta, P., and Riccio, A., *Catal. Lett.* **23**, 141 (1994).
15. Shelef, M., *Catal. Lett.* **15**, 305 (1992).
16. Hamada, H., Kintaichi, Y., Sasaki, M., and Ito, T., *Appl. Catal.* **64**, L1 (1990).
17. Kintaichi, Y., Hamada, H., Tabata, M., Sasaki, M., and Ito, T., *Catal. Lett.* **6**, 239 (1990).
18. Liu, D.-J., and Robota, H. J., *Appl. Catal. B: Environmental* **4**, 155 (1994).
19. Hamada, H., Kintaichi, Y., Sasaki, M., Ito, T., and Tabata, M., *Appl. Catal.* **70**, L15 (1991).
20. Halász, I., Brenner, A., and Ng, K. Y. S., *Catal. Lett.* **34**, 151 (1995).
21. Hoost, T. E., Laframboise, K. A., and Otto, K., *Catal. Lett.* **33**, 105 (1995).
22. Spoto, G., Zecchina, A., Bordiga, S., Ricchiardi, G., and Martra, G., *Appl. Catal. B: Environmental* **3**, 151 (1994).
23. Spoto, G., Bordiga, S., Scarano, D., and Zecchina, A., *Catal. Lett.* **13**, 39 (1992).
24. Komatsu, T., Ogawa, T., and Yashima, T., *J. Phys. Chem*. **99**(35), 13054 (1995).
25. Ukisu, Y., Sato, S., Abe, A., and Yoshida, K., *Appl. Catal. B: Environmental*, **2**, 147 (1993).
26. Yasuda, H., Miyamoto, T., and Misono, M., *in* "Reduction of Nitrogen Oxide Emissions" (U. S. Ozkan *et al*., Eds.). ACS Symposium Series, Vol. 587, p. 110. Am. Chem. Soc., Washington, DC, 1995.
27. Ukisu, Y., Sato, S., Muramatsu, G., and Yoshida, K., *Catal. Lett.* **11**, 177 (1991).
28. Bell, V. A., Feeley, J. S., Deeba, M., and Farrauto, R. J., *Catal. Lett.* **29**, 15 (1994).
29. Solymosi, F., and Bánsági, T., *J. Catal.* **156**, 75 (1995).
30. Valyon, J., and Hall, W. K., *J. Phys. Chem*. **97**, 1204 (1993).
31. Chao, C.-C., and Lunsford, J. H., *J. Am. Chem. Soc.* **93**, 71 (1971).
32. Chao, C.-C., and Lunsford, J. H., *J. Am. Chem. Soc.* **93**, 6794 (1971).
33. Odinokov, S. E., Mashkovsky, A. A., Glazunov, V. P., Iogansen, A. V., and Rassadin, B. V., *Spectrochim. Acta. Part A* **32**, 1355 (1976).
34. Claydon, M. F., and Sheppard, N., *Chem. Commun.*, 1431 (1969).
35. Odinokov, S. E., and Iogansen, A. V., *Spectrochim. Acta. Part A* **28**, 2342 (1972).
36. Bratos, S., *J. Chem. Phys.* **63**(8), 3499 (1975).
37. Bratos, S., and Ratajczak, H., *J. Chem. Phys.* **76**(1), 77 (1982).
38. Pelmenschikov, A. G., van Santen, R. A., Jänchen, J., and Meijer, E., *J. Phys. Chem*. **97**, 11071 (1993).
39. Jänchen, J., Peeters, M. P. J., van Wolput, J. H. M. C., Wolthuizen, J. P., van Hooff, J. H. C., and Lohse, U., *J. Chem. Soc. Faraday Trans.* **90**(7), 1033 (1994).
40. Cheng, J., Thomas, J. M., and Sankar, G., *J. Chem. Soc. Faraday Trans.* **90**(22), 3455 (1994).
41. Florián, J., and Kubelková, L., *J. Phys. Chem*. **98**, 8734 (1994).
42. Jentys, A., Worecka, G., Derewinski, M., and Lercher, J., *J.Phys. Chem*. **93**, 4937 (1989).
43. Pelmenschikov, A. G., and van Santen, R. A., *J. Phys. Chem*. **97**, 10678 (1993).
44. Dedecek, J., Sabolik, Z., Tvaruzková, Z., Kaucky, D., and Wichterlová, B., *J. Phys. Chem*. **99**, 16327 (1995).
45. Aylor, A., Larsen, S., Reimer, J., and Bell, A. T., *J. Catal.* **157**, 592 (1995).
46. Nakamoto, K., "Infrared and Raman Spectra of Inorganic and Coordination Compounds," 4th ed. Wiley–Interscience, New York, 1976.